Current Chemistry Letters 11 (2022) 341–352

Contents lists available at GrowingScience

Current Chemistry Letters

homepage: www.GrowingScience.com

Experimental study on the interaction of insulin with apatitic calcium phosphates analogous to bone mineral: adsorption and release

Abdelhadi El Rhilassi[a*] and Mounia Bennani-Ziatni[a]

[a]*Laboratory of Organic Chemistry, Catalysis and Environment, Department of Chemistry, Faculty of Sciences, Ibn Tofail University, BP 242, 14000, Kenitra, Morocco*

C H R O N I C L E

Article history:
Received February 30, 2022
Received in revised form
April 18, 2022
Accepted June 20, 2022
Available online
June 20, 2022

Keywords:
Apatite
Insulin
Adsorption
Kinetic
Isotherm

A B S T R A C T

The present work investigated the interaction of human insulin with synthesized poorly crystalline apatitic calcium phosphates containing simultaneously HPO_4^{2-} and CO_3^{2-} ions in various amount. The adsorption kinetics is very fast, while the release kinetics is generally slow. The chemical composition of apatite has an influence on both the adsorption and release processes. The experimental results show that the percentage of insulin adsorption and release decreased with the increase of the content of carbonate. The equilibrium adsorption data are fitted into Langmuir, Freundlich, Elovich, Temkin, and Dubinin–Radushkevich isotherms. The Langmuir model is best suited with a maximum monolayer adsorption capacity of 33.20 and 25.08 mg/g at 310 K corresponding to the carbonated and octocalcium phosphate apatite respectively. Isotherms parameters have revealed that the adsorption of insulin on these apatites is a feasible, spontaneous, and exothermic process. Fourier-transforms infrared confirm the fixation of insulin on non-carbonated and carbonated apatite. The adsorption and release of insulin molecules can be well described as an ions exchange-reaction between species in the hydrated layer of apatite and other species in solution. All of these results suggested that apatitic calcium phosphates can be used as systems for insulin delivery.

1. Introduction

Calcium phosphate -based biomaterials, especially poorly crystalline apatites are the inorganic compounds constituents of hard tissues in vertebrates.[1] Calcium phosphates present chemical and biological similarity with bones, teeth and other types of calcified tissues.[2] Due to biodegradability, bioactivity and osteoconductivity properties, biomaterials based on calcium phosphate are used in medicine for different applications, e.g., roofs of teeth and artificial bone, as well as a material for drug delivery systems.[3-6] In addition, calcium phosphates can be used for controlled release systems due to their high affinity to various active agents.[7]

Human insulin is used to treat diabetic diseases by using various methods such as direct injection and system pumping.[8-10] So far, the search for other simple and non-invasive methods is desirable and necessary. Much research focuses on the adsorption and release of organic molecules of different sizes such as amino acids and proteins by the apatitic calcium phosphates[11-14]. For this reason, the interaction of insulin with supports such as calcium phosphate will be the objective of this research subject in order to understand the adsorption and release processes for the development of surfaces intended for the administration of this therapeutic protein.

Poorly crystalline apatites are covered with a hydrated layer containing ions, such as Ca^{2+}, HPO_4^{2-} and CO_3^{2-}, their composition may vary in the domain in which the Ca/P atomic ratio is between 1.33 and 1.67. These apatites are analogous

* Corresponding author. Tel : +212 6 62 13 13 72
E-mail address aelrhilassi@gmail.com (A. El Rhilassi)

doi: 10.5267/j.ccl.2022.6.003

to bone mineral and are deficient in calcium ion in which the carbonate ions CO_3^{2-} substitutes the hydrogenophosphate ions HPO_4^{2-}according to the general chemical formula[15] :

$$Ca_{(8+0.57b)}[PO_4]_{(3.5+1.64b)}[HPO_4]_{2.5(1-b)}[CO_3]_{0.86b}OH_{0.5(1-b)} \text{ with } 0 \leq b \leq 1.$$

In the present, work we are interested in using two apatites ; Octocalcium phosphate apatitic (OCPa) for Ca/P=1.33 of composition : $Ca_8(PO_4)_{3.5}(HPO_4)_{2.5}OH_{0.5}$ and Carbonated calcium phosphate apatite (CCPa) for Ca/P=1.48 of composition : $Ca_{8.27}(PO_4)_{4.28}(HPO_4)_{1.3}(CO_3)_{0.41}OH_{0.26}$. The capacity of retention and release of these biomaterials have been tested for human insulin under physiological conditions. The chemical composition of apatitic calcium phosphates is well considered as an experimental factor realized in order to establish a relation between adsorption and release processes with the surface characteristic of these apatitic compounds. The Langmuir, Freundlich, Elovich, Temkin, and Dubinin–Radushkevich models are used to describe equilibrium isotherms. Isotherm parameters are also calculated to establish the mechanism of adsorption. The physical and chemical characterizations of apatites are conducted by different methods such as X-ray diffraction (XRD), Energy dispersive X-ray (EDX) and Fourier-transform infrared (FTIR), the potential of the apatites are evaluated for adsorption and release of insulin.

This work contributes to specifying the role of the parameters which involve in the interaction of insulin with various apatitic calcium phosphates and helps to explain the mechanism of this interaction under physiological conditions.

2. Materials and methods

2.1 Adsorbents

Poorly crystalline apatitic calcium phosphates are synthesised by a double decomposition process in water–ethanol at 310 K.[15] The powders obtained are characterized by physicochemical analysis.[16] The calcium content is determined by complexometry with Ethylene Diamine Tetra Acetic Acid (EDTA), the phosphate ion content by spectrophotometry of phospho-vanado-molybdic acid and carbonates ion by volumetric. The relative error on the level of calcium, phosphate and carbonate is 0.5%. The determination of the atomic Ca/P ratio of the precipitate had a relative error of 1%. The specific surface area is determined by the BET method, the result obtained is 58 m^2/g for OCPa and 95 m^2/g for CCPa, with an error of 5 %.

Fourier-transform infrared spectroscopy spectra are determined using 89 VERTEX 70/70V FT-IR spectrometers (Bruker Optics). The infrared spectra of synthesized OCPa (**Fig. 1**) and CCPa (**Fig. 2**) in 4000–400 cm^{-1} region show the main peaks characteristics of apatitic calcium phosphates. The most characteristic chemical groups are given in **Table 1**.

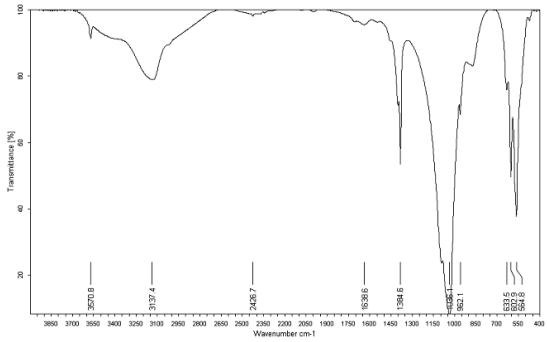

Fig. 1. FTIR spectra of OCPa

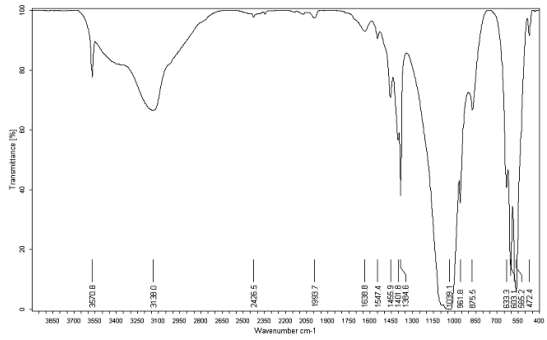

Fig. 2. FTIR spectra of CCPa

Table 1. FTIR absorption bands of synthesized OCPa and CCPa chemical groups.

OCPa		CCPa	
Chemical groups	Absorption bands, (cm^{-1})	Chemical groups	Absorption bands, (cm^{-1})
OH^-	3570.8 ; 633.5	OH^-	3570.8 ; 633.3
HPO_4^{2-}	875	HPO_4^{2-}	875
PO_4^{3-}	1036.1 ; 962.1 ; 602.9 ; 564.8 ; 474	PO_4^{3-}	1039.1 ; 961.8 ; 603.1 ; 565.2 ; 472.4
H_2O	2600 -3600 ; 638.6	H_2O	2600 - 3600 ; 1638.8
		CO_3^{2-}	1547.4 ; 1455.9; 1401.8

The XRD patterns of synthesized OCPa (**Fig. 3**) and CCPa (**Fig. 4**) are conducted using an X-ray diffractometer X'PERT. The positions, interreticular distances and intensities of the peaks are summarized in **Table 2**. The apatites yielded broad and overlapping reflections, indicating their low crystallinity.

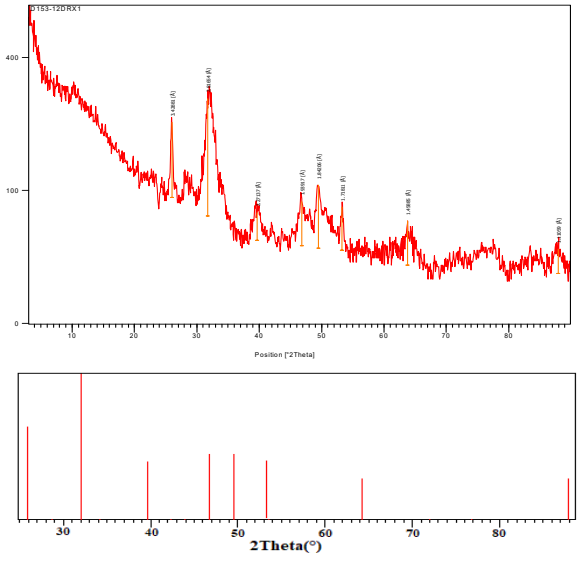

Fig. 3. XRD pattern of OCPa

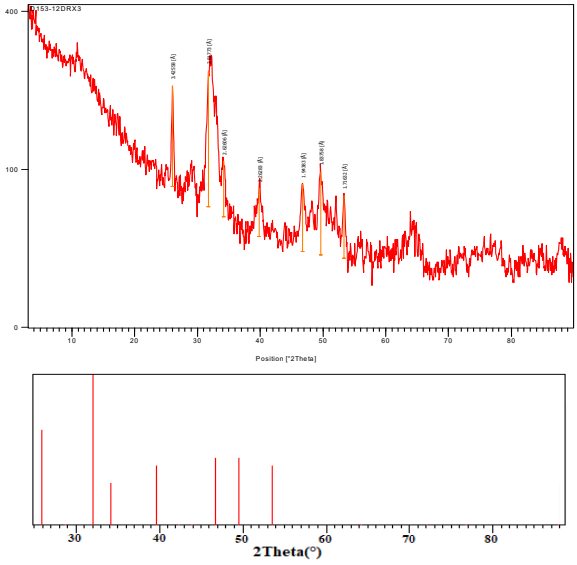

Fig. 4. XRD pattern of CCPa

Table 2. Positions, interreticular distances and intensities of the peaks of diffraction of OCPa and CCPa.

OCPa			CCPa		
Pos. [°2Th.]	d-spacing [Å]	Rel. Int. [%]	Pos. [°2Th.]	d-spacing [Å]	Rel. Int. [%]
25.9871	3.42881	63.23	26.0120	3.42558	75.09
31.7713	2.81654	100.00	31.7575	2.81773	100.00
39.6824	2.27137	13.62	34.1438	2.62606	30.05
46.8514	1.93917	22.70	39.8386	2.26283	21.46
49.4823	1.84206	34.60	46.7326	1.94383	28.77
53.2745	1.71811	21.21	49.6111	1.83758	36.63
63.8024	1.45885	18.16	53.3345	1.71632	24.43

The energy dispersive X-ray (EDX) analysis (**Fig. 5**) confirmed the presence of relevant elements O, P and Ca in OCPa, and O, P, Ca and C in CCPa. The intensity of these peaks is proportional to the chemical composition of these two apatites.

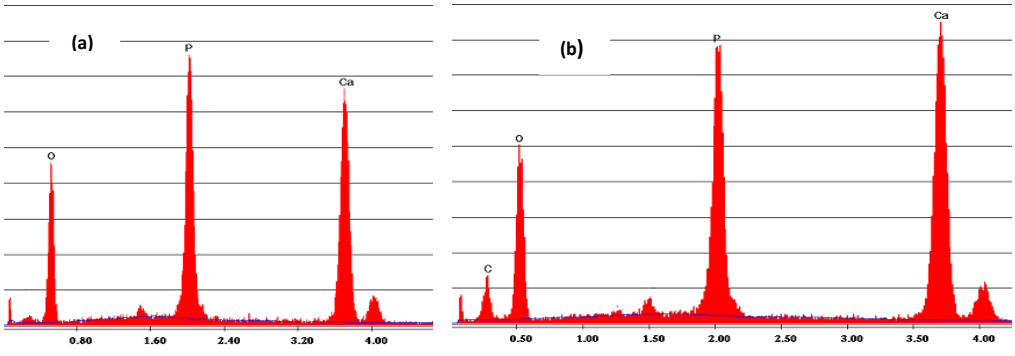

Fig. 5. EDX spectra of (a): OCPa, (b) CCPa

The pH of the zero point charge (pH_{ZPC}) is a parameter that plays an important role in the interaction between adsorbate and adsorbent. It corresponds to the equality between the negative charges and the positive charges appearing on the surface of a solid in contact with a polar liquid phase.[17] In order to determine the pH_{ZPC} of the apatites, 0.2 g apatite powder placed in beakers containing 20 mL of 0.01 M NaCl solutions. The initial pH of these solutions is adjusted from 4 to 10 by adding sodium hydroxide solution (0.1 M) or hydrochloric acid solution (0.1 M). After 48 h of stirring at ambient temperature, the final pH is measured. The pH corresponding to the point of intersection of $\Delta pH = pH_{(final)} - pH_{(initial)}$ with the axis $pH_{(final)} = pH_{(initial)}$ is the pH_{PCZ} of the apatite. In the present study, the pHpzc of the OCPa and CCPa are found to be 5.74 and 5.94 respectively (**Fig. 6**).

Generally, when the pH value of the solution is lower than pH_{ZPC}, the surface of the adsorbent is positively charged and the opposite for pH value higher than pH_{ZPC}, the surface is negatively charged.

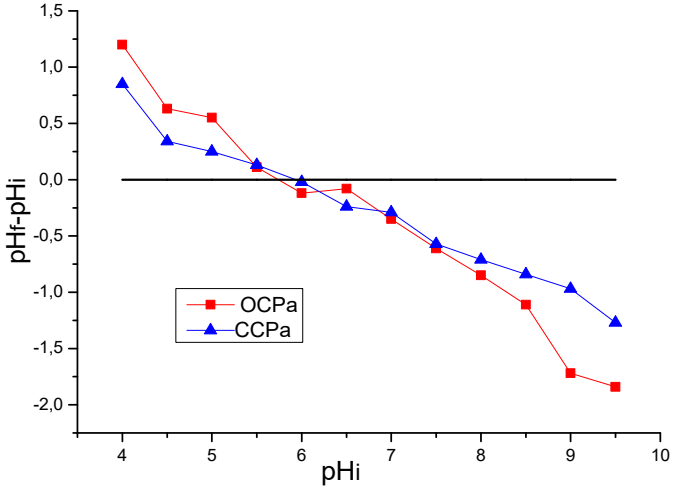

Fig. 6. pH_{ZPC} of OCPa and CCPa

2.2 Adsorbates

The adsorbate used in this paper is biosynthetic human insulin (rDNA origin) from Novo Nordisk A/S (Bagsvaerd, Denmark). The insulin has the empirical formula $C_{257}H_{383}N_{65}O_{77}S_6$, a molecular weight of 5807.57±0.299 Da, and a pI (pH isoelectric) of 5.4 ±0.05. The samples of adsorbates are prepared from the stock solution of 3500 mg/l using physiological saline (NaCl 9g/l) and stored at 4°C. The infrared spectrum of insulin (**Fig. 7**) show two characteristic absorption peaks one at ~1660 cm^{-1} for amide I and another at ~1516 cm^{-1} corresponding to amide II mainly due to carbonyl group C=O stretching vibration characteristic of the protein spectrum.[18-21]

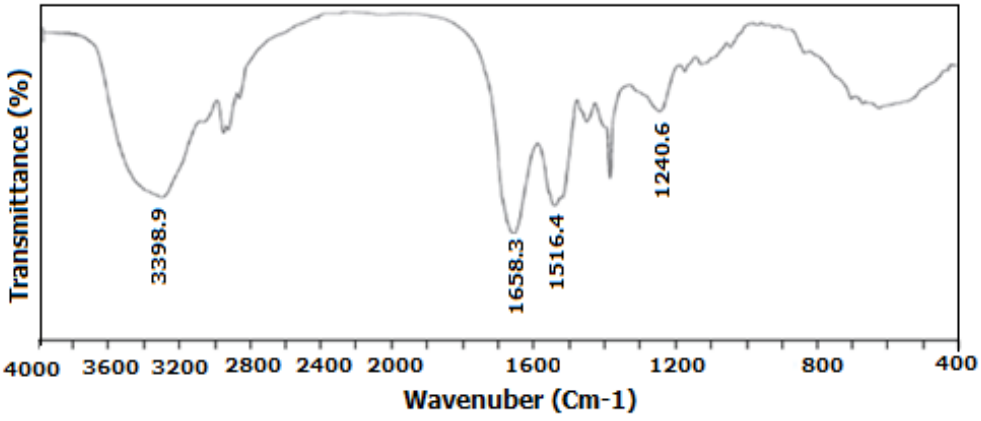

Fig. 7. FTIR spectrum of human insulin

2.3 Experimental protocol

Adsorption is performed in batch experiments by adding 1ml of the insulin solution to a test tube containing 20 mg of powder calcium phosphate. After stirring for 1 min at the speed of 1000 rpm, the mixture of adsorbate and adsorbent is placed in a thermostatic bath at a physiological temperature of 37°C for different contact times. The amount of adsorbed insulin per unit of apatite mass is calculated using Eq. (1):

$$Q_{ads}(mg/g) = \frac{V\,(C_0 - C)}{m} \tag{1}$$

where C_0 and C are respectively the initial and residual concentration of insulin (mg/ml), V is the volume of solution (l) and m is the mass of adsorbent used (g). The percentage of insulin adsorption (%) is calculated according to Eq. (2):

$$\%ads = \frac{(C_0 - C)}{C_0} \times 100 \tag{2}$$

The release experiments are performed using the following method; 1 mL of physiological saline (NaCl 9 g/L) is added to a test tube containing 20 mg of the apatite previously adsorbed of insulin. The amount of released insulin per unit of apatite mass is calculated from the following Eq. (3):

$$Q_{rel}(mg/g) = C_{rel} \times \frac{V}{m}, \quad (3)$$

where C_{rel} is the equilibrium concentration of the insulin released in solution (mg/ml), V is the volume of the solution (1 ml), and m is the mass of the apatite used (20 mg). The percentage of insulin release is determined using Eq. (4):

$$\%rel = \frac{Q_{rel}}{Q_{ads}} \times 100 \quad (4)$$

After treatment, the solid and solution are separated by fritted glass N°4. The supernatants obtained are examined by measuring the pH and determining the equilibrium concentration using a UV–vis spectrophotometer (Model 3100, Japan) at 540 nm. The collected solids are dried in the oven at 80 ◦C for 24 h and solutions are stored at 4 °C.

3. Results and discussion

3.1 Study of Adsorption

3.1.1 Adsorption kinetics

Experimental results of adsorption of the insulin with initial concentration 3500 mg/l by OCPa and CCPa for contact time 15 min to 24 h at 310 K are reported in **Fig. 8**. Adsorption kinetics is fast; the maximum adsorption is observed in the early minutes of contact and the equilibrium is reached after about 0.5 hours of incubation. The fast adsorption may be due to the many active sites available at the beginning of the adsorption process. The formation of plateau within a few minutes indicates also that the phosphates are very effective adsorbents for the administration of this drug.

The adsorption process is influenced by the chemical composition of the adsorbent. Indeed, the adsorption rate decreases with an increase in the initial Ca/P atomic ratio of apatite; e.g, it passes from 87.11% for OCPa of Ca/P= 1.33 containing more HPO_4^{2-} ions and exempt CO_3^{2-} ions to 73.43% for CCPa of Ca/P= 1.48 containing $CO_3^{2-}$and HPO_4^{2-}ions.

It is noticed that the pH values of solutions after adsorption kinetics are between 6.04 and 7.2 (**Fig. 9**). The pH may vary as a function of contact time and of the type of adsorbent used. It decreases with increasing of contact time and with decreasing of the Ca/P ratio of apatite. Moreover, these values are above the point of zero charge (pH_{pzc}); which shows that the global charge of the surface of the apatites used is negative. Therefore, the adsorption process may be due to the interaction between the negatively charged surface of apatites and insulin molecules.

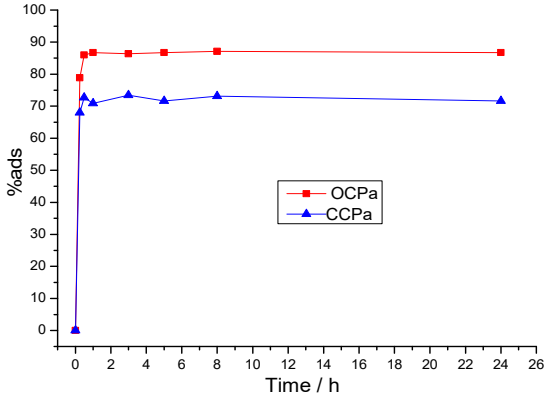

Fig. 8. Adsorption rate (%) of insulin onto OCPa of Ca/P= 1.33 and CCPa of C/P=1.48

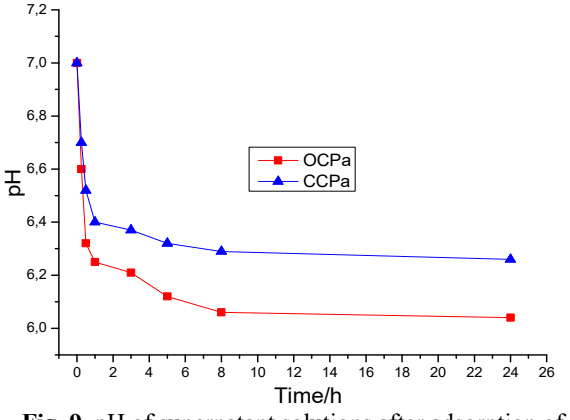

Fig. 9. pH of supernatant solutions after adsorption of insulin onto OCPa and CCPa

3.1.2 Adsorption isotherms

The relationship between the adsorbate in the liquid phase and the adsorbate adsorbed on the surface of the adsorbent at equilibrium at a constant temperature is described by the adsorption isotherm. In the present study, adsorption isotherms are studied at physiological temperature 310 K, on insulin solutions with varying concentrations from 350 to 3500 mg/l, and a contact time of 5 hours, time is taken to reach equilibrium. In order to determine the amount maximum of insulin adsorbed under the experimental conditions used, it is important to study the various adsorption isotherm models and verify which model presented the best adjustment of the experimental equilibrium data. The data are fitted into the following

isotherms: Langmuir,[22] Freundlich,[23] Elovich,[24] Temkin[25] and Dubinin-Raduskevich.[26] Hypotheses and values of the parameters of each model for the adsorption of insulin onto OCPa and CCPa are given in **Table 3**. The evolution of the amount adsorbed Q_{ads}(mg/g) of insulin as a function of its equilibrium concentration C_e (mg/l) is represented in **Fig. 10**. We can notice that this amount increases quickly for low concentrations in solution and then reaches a plateau; this can be explained by the formation of a monolayer adsorption type, which is described by the classical Langmuir model.

Langmuir adsorption parameters are determined by the following Eq. (5):

$$C_e/Q_{ads} = 1/b\,Q_\infty + C_e/Q_\infty\,, \tag{5}$$

where C_e (mg/l) is the equilibrium concentration of the adsorbate, Q_{ads} (mg/g) is the amount of adsorbed insulin per unit of adsorbent mass, Q_∞ (mg/g) and b (l/g) are Langmuir constants related to sorption capacity and rate of sorption, respectively. **Fig. 11** represents the experimental data of C_e/Q_{ads} versus C_e at 310 K. The values of Q_∞ and b are computed from the slope and intercept, respectively, of the isothermal line and they are listed in **Table 3**. The insulin adsorption capacity, Q_∞ (mg of insulin per g of apatite), which is a measure of the maximum adsorption capacity corresponding to complete monolayer coverage, has been influenced by the chemical composition of apatite; e.g., its value was decreased from 33.20 to 25.07 mg/g, while the Ca/P atomic ratio increased from 1.33 for OCPa to 1.48 for CCPa. We noted that the constant of sorption $b(l/g)$ increases when the Ca/P increases also, it passes from 3.41 for OCPa to 3.63 for CCPa, the compound which contains more carbonate ions and fewer hydrogenophosphate ions. The increase of this parameter can be explained by the increase of the specific surface which passes from 58 m^2/g for OCPa to 85m^2/g for CCPa.

The essential characteristic of the Langmuir isotherm can be expressed by a dimensionless constant called the separation factor R_L, defined by Weber and Chakravorti[27] according to the following Eq. (6):

$$R_L = \frac{1}{1} + b\,C_0\,, \tag{6}$$

where C_0 is initial concentration of insulin and b is the Langmuir constant. This factor show the type of isotherm to be either linear ($R_L = 1$), irreversible ($R_L = 0$), favourable ($0 < R_L < 1$ or unfavourable ($R_L > 1$). **Fig. 12** represents the evolution of the estimated value of R_L depending on the initial concentration of nsulin in the solution. We found that R_L is lying between 0 and 1 indicating the favorable conditions for adsorption at physiological temperature. The R^2 correlation coefficient values (98.78 for OCPa and 99.73 for CCPa) prove that the data fitted well to the Langmuir Isotherm model under the concentrations range studied (**Table 4**).

A temperature studied, the free energy of adsorption $\Delta G^0_{ads}(J/mol)$ can be calculated by the following equation [28]:

$$\Delta G^0_{ads} = -RT\,Ln\,b\,, \tag{7}$$

where b(l/g) is the adsorption equilibrium constant obtained from Langmuir isotherm, T is the absolute temperature in Kelvin, and R is the universal gas constant ($8.314\,J\,mol^{-1}K^{-1}$). The thermodynamic parameter, ΔG^0, is shown in **Table 3**. The negative values found of ΔG^0_{ads} confirm the spontaneous nature of the adsorption process with a high preference for insulin to adsorb onto OCPa and CCPa. Moreover, these values are between −20 KJ/mol and 0 KJ/mol indicating that the insulin adsorption process should be regarded as physical adsorption.[29]

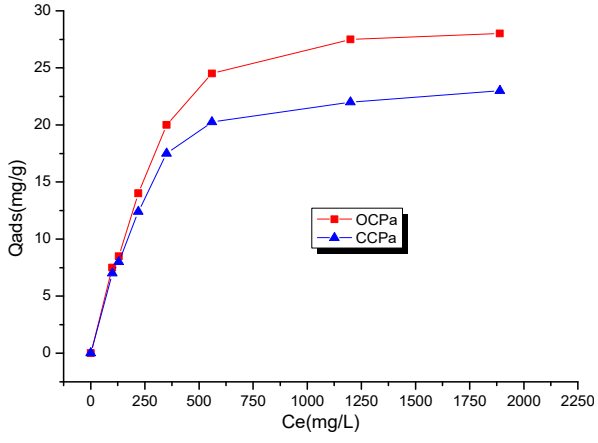

Fig. 10. Adsorption isotherms of insulin onto OCPa and CCPa (solid quantity : 200 mg, stirring time : 1 min, T : 310 K)

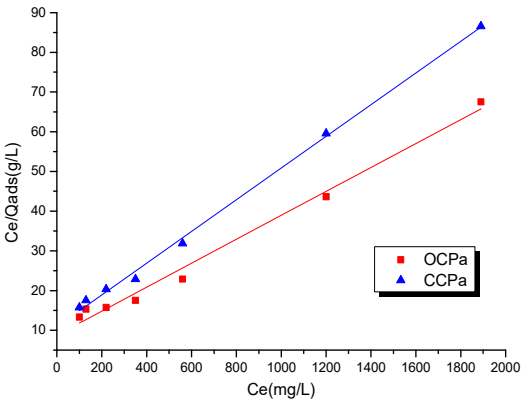

Fig. 11. Langmuir isotherm model

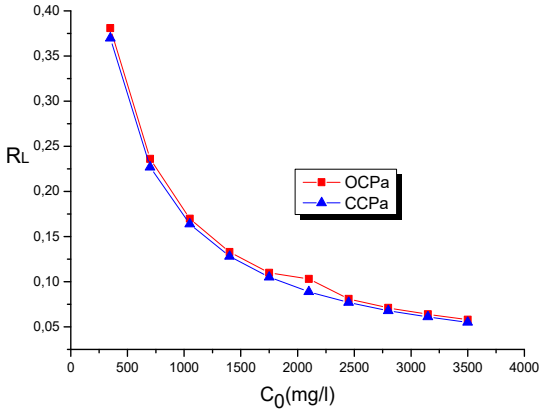

Fig. 12. Evolution of the estimated value of R_L

The linearized form of the Freundlich model is expressed by the empirical Eq. (8):

$$Ln\ Q_{ads} = Ln\ a + m\ Ln\ Ce, \tag{8}$$

where $a(mg^{1-m}g^{-1}l^m)$ and m are Freundlich constants and represent the adsorption capacity of adsorbent and adsorption intensity, respectively. These parameters must be calculated from the slope and intercept, respectively, of a graph of LnQ_{ads} against $LnCe$ (**Fig. 13**). The values of a , m and the coefficients of determination, R^2, are shown in **Table 3**. According to the literature[30], the value of m in the range of 0.1–0.5 indicates good, 0.5–1 moderately difficult, and greater than 1 poor adsorption characteristics. From the data in **Table 3**, the values of m are below one and in the range of 0.1–0.5 indicating that the adsorption of insulin is favorable and good by OCPa and CCPa. This result is in agreement with that of the R_L value.

The linearized form of the Elovich model is defined by Eq. (9):

$$Ln\ (Q_{ads}/C_e) = Ln\ (K_E\ Q_\infty) + Q_{ads}\ /Q_\infty\ , \tag{9}$$

where Q_∞ (mg/g) is the maximum theoretical amount of adsorbate adsorbed per unit mass of adsorbent and $K_E(l/g)$ is the Elovich adsorption constant related to the affinity of the surface sites with the adsorbate. **Fig. 14** represents the experimental data of $Ln\ (Q_{ads}/C_e)$ versus Q_{ads} at 310 K. The values of Q_∞ and K_E are calculated from the slope and intercept, respectively, of the isothermal line and they are listed in **Table 3**. We note that the Q_∞ decreased from 16.49 to 14.80 mg/g as the Ca/P increased from 1.33 to 1.48.

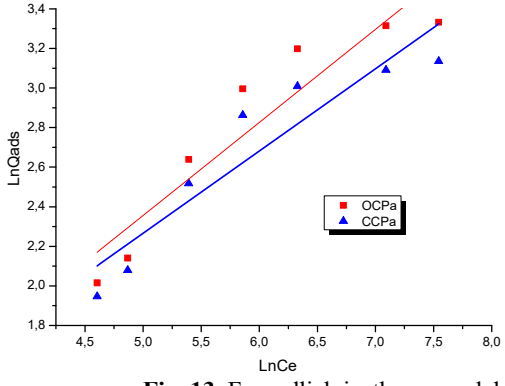

Fig. 13. Freundlich isotherm model

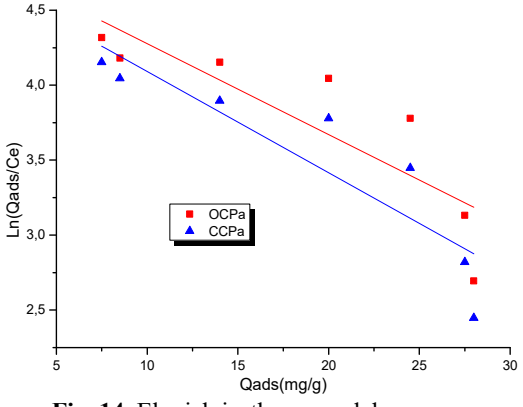

Fig. 14. Elovich isotherm model

The linearized form of the Temkin model is given by the following Eq. (10):

$$Q_{ads} = (R\ T/b_t)\ Ln\ a_t + (R\ T/b_t)\ Ln\ C_e \tag{10}$$

where R is the universal gas constant (8.314 J mol^{-1} K^{-1}), T is the temperature at 310 K, b_t is the Temkin isotherm constant associated to the heat of adsorption (J mol^{-1}) and a_t is the Temkin isotherm constant (l/g). The parameters of Temkin model b_t and a_t are determined from the slope and intercept, respectively, of the plot of Q_{ads} against $Ln\ Ce$ (**Fig. 15**) and are listed in **Table 3**. The values found of b_t corresponding to OCPa and CCPa are 0.337 and 0.444 KJ.mol^{-1} respectively.

The positive value of this parameter means that the adsorption process is exothermic. In addition, the low values of b_t suggest that the adsorption of insulin on the OCPa and CCPa can be considered as a purely electrostatic process.

The linearized form of the Dubinin–Radushkevick (D–R) model is given by the following Eq. (11):

$$Ln\ Q_{ads} = Ln\ Q_{DR} - B_{DR}\ \varepsilon^2\ , \tag{11}$$

where $Q_{DR}(mg/g)$ is the theoretical isotherm saturation capacity related to mean sorption energy, $B_{DR}(mol^2/J^2)$ is the D–R model constant and ε is the Polanyi potential can be calculated as :

$$\varepsilon = R\ T\ Ln(1 + 1/C_e)\ , \tag{12}$$

where R and T represent the gas constant (8.314 J/mol.K) and absolute temperature (310 K), respectively. This model is used to distinguish the chemical and physical adsorption with its mean free energy of adsorption, $E(KJ/mol)$, which can be considered as the energy required to transfer one mole of molecule from infinity in solution to the surface of the solid particles. Its value can be evaluated from the following equation :

$$E = \frac{1}{\sqrt{B_{DR}}} \tag{13}$$

The values of B_{DR} and Q_{DR} calculated by plotting $Ln\ Q_{ads}$ versus ε^2 (**Fig. 16**) and E are given in **Table 3**. It can be found that the value of Q_{DR} decreased from about 24 to 20 mg/g, while the Ca/P atomic ratio increased from 1.33 for OCPa to 1.48 for CCPa. This is in great agreement with the findings regarding to Q_∞ the values obtained for the Langmuir isotherm model. The values obtained of E are 15.58 and 16.44 J/mol, respectively, for OCPa and CCPa. In the literature,[31] the E value ranges from 1.0 to 8.0 KJ/mol for physical adsorption and from 9.0 to 16.0 KJ/mol for chemical ion-exchange adsorption.[31] Therefore, these results indicate that the adsorption of insulin onto OCPa and CCPa may be attributed to the physical adsorption mechanism, which is in agreement with the above study.

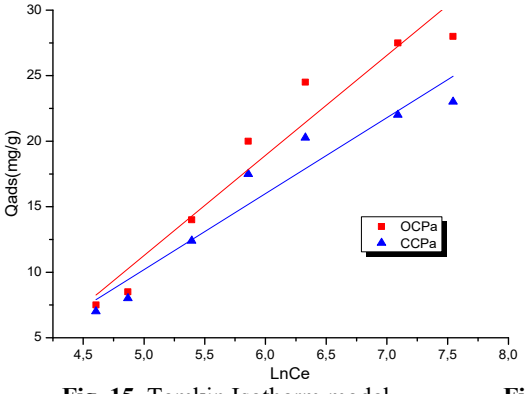

Fig. 15. Temkin Isotherm model

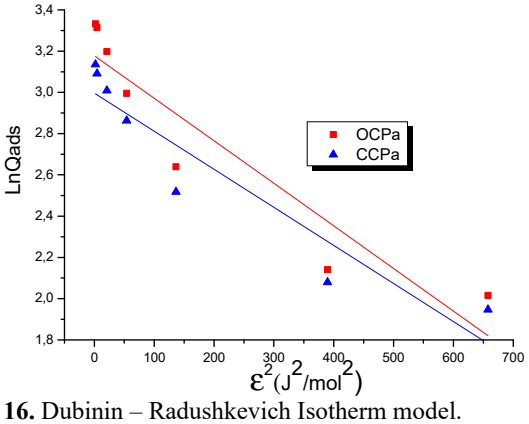

Fig. 16. Dubinin – Radushkevich Isotherm model.

Table 3. Hypotheses and values of the parameters of Langmuir, Freundlich, Elovich, Temkin and Dubinin–Radushkevich models for the adsorption of insulin onto OCPa and CCPa.

Models	Hypotheses	parameters	OCPa	CCPa
Langmuir	- monolayer, - finite number of adsorption sites, - one molecule per site, - no mobility of the molecules and no interaction.	b(l/g)	3.41	3.63
		Q_∞(mg/g)	33.20	25.08
		R^2(%)	98.78	99.73
		$\Delta G^0_{ads}(KJ/mol)$	-3.16	-4.01
Freundlich	- heterogeneous surface, - no mobility of the molecules on the surface and no interaction.	a(mg^{1-m} g^{-1} l^m)	1.003	1.203
		m	0.471	0.416
		R^2(%)	86.18	84.98
Elovich	- variable number of sites adsorption, - multilayer adsorption.	Q_∞(mg/g)	16.49	14.80
		K_E(l/mg)	8.01	7.94
		R^2(%)	68.28	77.53
Temkin	- adsorbate -adsorbate interactions, - heat of adsorption (b_t) varies linearly with the degree of coverage of the adsorbent.	b_t(KJ.mol^{-1})	0.337	0.444
		a_t(l/g)	0.029	0.039
		R^2(%)	93.24	91.88
Dubinin – Radushkevich (D-R)	-heterogeneous and homogeneous surface, -the adsorption follows a pore-filling mechanism.	E(J.mol^{-1})	15.58	16.44
		B_{DR}(mol^2/J^2)	2.06.10^{-3}	1.85.10^{-3}
		Q_{DR}(mg/g)	24.003	20.026
		R^2(%)	85.93	87.36

Analysis of **Table 3** shows that the Langmuir model is the most appropriate for the fit of the equilibrium experimental data of adsorption of insulin on the OCPa and CCPa (higher value of coefficient of determination) as compared to Temkin, Freundlich, Elovich, and Dubinin-Radushkevich models under the concentration range studied and in the temperature of 310K.

3.1.3 Solid (FTIR)

Fourier transform infrared spectrophotometry is used to study the interaction between apatite and insulin. **Fig. 17** and **18** presents the FTIR spectra of synthetic OCPa and CCPa after adsorption in 3500 mg/l of insulin in 5h contact time. In addition to the peaks attributed to apatites OCPa and CCPa, these spectra are illustrated with other major peaks in the region 1400 -1700 cm^{-1} characteristic of insulin. The peak at 1455 cm^{-1} is due to the bending vibration of CH_2.[32] The OCPa spectrum (**Fig. 17**) shows two absorption peaks one at 1663.3 cm^{-1} for amide I and another at 1538.9 cm^{-1} corresponding to amide II due to carbonyl group C=O stretching vibration characteristic of the insulin, these peaks are displaced for CCPa at 1661.1 cm^{-1} and 1545.9 cm^{-1}, respectively (**Fig. 18**). It appears, in the 3670–3300 cm^{-1} region, the band attributed to the stretching vibration of the NH_2 and NH groups.[33,34]

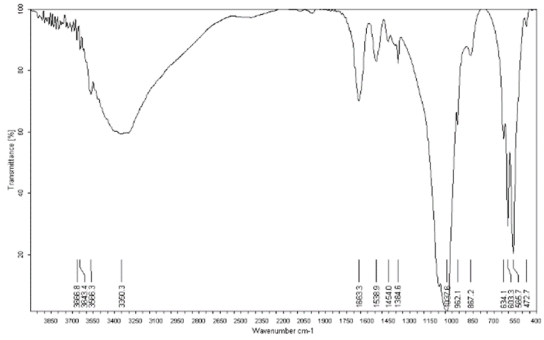

Fig. 17. FTIR spectra of OCPa after adsorption in 3500 mg/l of insulin

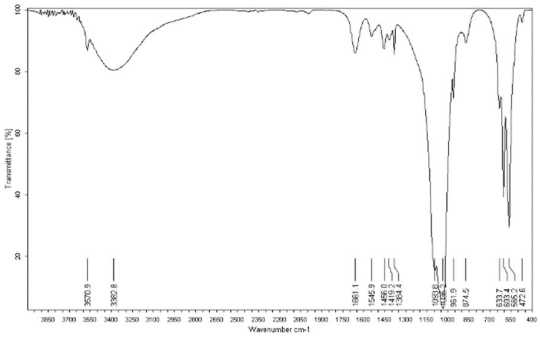

Fig. 18. FTIR spectra of CCPa after adsorption in 3500 mg/l of insulin

3.2 Study of Release

This study is carried out in vitro to examine the insulin's release kinetics, which is previously adsorbed onto OCPa and CCPa for contact times: 0.25 to 24 hours (**Fig. 19**) at 310 K. It is found that the release process is very fast in the first minutes and slows down after about 2 hours. We also noticed that the release process of insulin is influenced by the chemical composition of apatite. Indeed, the release rate is about 48.4% for OCPa compound free from carbonate CO_3^{2-}ions and presents the maximum of HPO_4^{2-}ions and about 37.8% for CCPa compound containing both $CO_3^{2-}$and HPO_4^{2-}ions.

pH values of solutions after the release of insulin previously adsorbed onto OCPa and CCPa are between 5.96 and 6.23. These values are nearly more than the point of zero charge (pH_{pzc}) of the apatites, and that may explain their anionic surface. We noticed that the high pH value corresponds to the maximum rate (%) of insulin release (**Fig. 20**). The evolution in pH versus time can be explained by a phenomenon of ions exchange between apatite surface previously adsorbed insulin and the surrounding environment similar to the biological fluid.

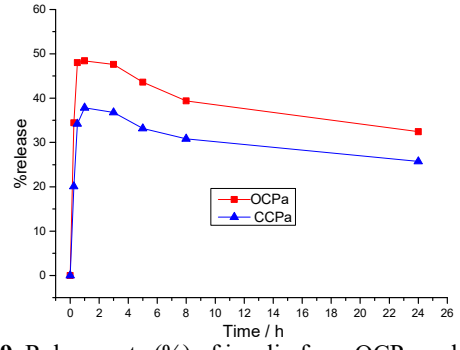

Fig. 19. Release rate (%) of insulin from OCPa and CCPa

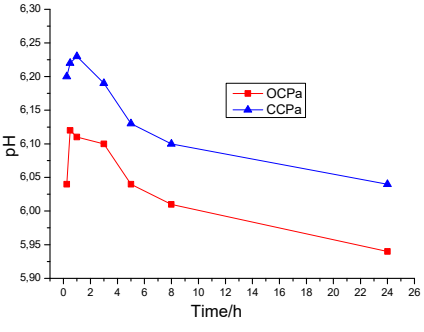

Fig. 20. pH of supernatant solutions after release of insulin onto OCPa and CCPa

3.3 Apatite–insulin interactions

Due to the presence of significant amounts of bivalent ions, $HPO_4^{2-}$and CO_3^{2-} ions and deficiency in calcium ions, the synthetic poorly crystalline apatitic calcium phosphate is considered as a model mineralized biological and non-stoichiometry. The general chemical formula proposed of this model is : $Ca_{(8+0.57b)}[PO_4]_{(3.5+1.64b)}[HPO_4]_{2.5(1-b)}[CO_3]_{0.86b}OH_{0.5(1-b)}$ with $0 \leq b \leq 1$. The synthetic apatite is covered with the hydrated layer which contains loosely bound mobile ions (Ca^{2+}, $HPO_4^{2-}$and CO_3^{2-}) and insulin previously adsorbed (**Fig. 21**).

The hydrated layer which is located between the apatite domain and solution plays an important role in the apatite–insulin interactions. Indeed, The ions of the hydrated layer of apatites can be exchanged by ions of the solution or ionic end groups of insulin. Due to the very high specific surface area and high reactivity of apatites, the insulin previously adsorbed can be released. The reactions adsorption-release of insulin involving the hydrated layer are spontaneously, reversibly, and can be considered as electrostatic interactions.

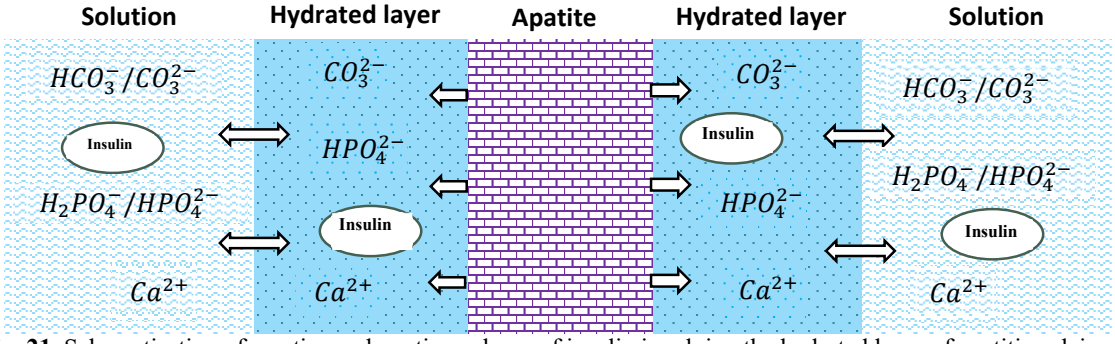

Fig. 21. Schematisation of reactions adsorption-release of insulin involving the hydrated layer of apatitic calcium phosphate

4. Conclusion and Perspective

The adsorption and release kinetics process attest to the high interaction between apatitic calcium phosphates of low crystallinity with Ca/P 1.33 and 1.48 analogous to bone minerals and various functional groups of insulin under physiological conditions. Indeed, the interaction process was very fast in the first minutes, the decrease in release rate might be due to the existence of a re-adsorption reaction between the apatite surface and insulin previously released in the solution. In addition, the percentage of insulin adsorbed is higher than that released in solution, which explains the high apatites reactivity related to their high specific surface area that can interact with the functional groups of insulin.

The results of Fourier-transform infrared spectroscopy confirm the fixation of insulin with apatites used; the spectra reveal, in addition to bands of the apatites examined, specific bands of amide I and amide II constituting the peptide bond of the insulin structure. The adsorption and release reactions are strongly affected not only by the chemical properties of the insulin but also by the chemical composition of apatite used; the rate of these reactions decreases with the increase of the number of carbonate ions and with the decrease of hydrogenophosphate ions in the prepared apatite. Under physiological conditions, the pH result of the incubation medium of adsorption and release reaction is higher than that of the isoelectric point (PI=5.4) of insulin and higher than the point of zero charge (pH_{pzc}) of apatite, which shows that the insulin molecules and the apatites surface used are negatively charged. Due to these reasons, the interaction processes reveal, in this case study, an ion-exchange mechanism involving the replacement of mineral ions of the apatites surface (negatively charged functional groups) by insulin molecular ions from the solution. Therefore, the adsorption of insulin on apatitic calcium phosphates is considered to obey to electrostatic interactions. The possible surface exchange reactions mechanism for the interaction of molecular ions of insulin with apatitic calcium phosphates can be hypothesized as below:

$$\textit{Adsorption:} \quad (Ins)_{sol} + (G)_{Apt} = (Ins)_{Apt} + (G)_{Sol}$$
$$\textit{Release:} \quad (Ins)_{Apt} + (G)_{Sol} = (Ins)_{sol} + (G)_{Apt}$$

with $(Ins)_{Sol}$ and $(Ins)_{Apt}$ are the insulin in an ionic state in solution and on the apatite surface respectively. $(G)_{Apt}$ and $(G)_{Sol}$ are the apatite group in an ionic state on the apatite surface and in solution respectively.

In addition to this hypothesis, the functional groups charged negatively are more than the positive groups on the surface of these apatites. Therefore, the interaction process may be involved the anionic groups of insulin and both the calcium sites and anionic groups of apatite, it is considered a physical interaction. This is in accordance with the previous study,[8] which shows that the interaction of amino acids with apatites is governed by electrostatic interactions. Furthermore, the slight variation in pH of solution supernatant after adsorption and release processes may be caused by a reaction exchange between

the insulin molecules in solution or those previously fixed on poorly crystalline apatitic calcium phosphates and labile ions, such as Ca^{2+}, HPO_4^{2-}, $H_2PO_4^-$ and CO_3^{2-}, at the interface of hydrated surface particles.

In order to identify the isotherm that best represents the adsorption of insulin onto the OCPa and CCPa, experimental data are fitted to five models: Langmuir, Freundlich, Elovich, Temkin, and Dubinin-Radushkevich. Analysis of the results shows that the best description of the adsorption phenomenon is correlated well with the Langmuir model under the concentration range studied with the highest correlation coefficient value of 99.73. However, the other models all have a low R-squared value, between 68.28 and 93.84. The monolayer adsorption capacity according to the most dominant model, Langmuir, is 33.20 mg/g for OCPa and 25.08 mg/g for CCPa. The isotherm parameters revealed that the adsorption process is favorable, exothermic, spontaneous in nature, and confirmed that this adsorption is controlled by physisorption.

The results obtained show that the poorly crystalline apatitic calcium phosphates provide a significant advantage over the interaction induced by insulin. It is possible to develop new perspectives by adapting drug delivery tools, such as pellets of apatitic calcium phosphates, which can be used as a support for the release of insulin.

Acknowledgement

The authors would like to express my sincere gratitude to all laboratory members and my family for their help to realize this research topic.

References

1 Vallet-Regi M., and Gonzalez-Calbet J. M. (**2004**) Calcium phosphates as substitution of bone tissues. *Prog. Solid State Chem.*, 32 (1-2) 1-31.
2 Dorozhkin S. V. (**2013**) A detailed history of calcium orthophosphates from 1770s till 1950. *Mater. Sci. Eng. C.*, 33 (6) 3085-3110.
3 Hakim L. K., Yazdanian M., Alam M., Abbasi K., Tebyaniyan H., Tahmasebi E., Khayatan D., Seifalian A., Ranjbar R., and Yazdanian A. (**2021**) Biocompatible and Biomaterials Application in Drug Delivery System in Oral Cavity. *Evid. Based Complement. Alternat. Med.*, (12) 9011226.
4 Narwade V. N., Pottathara Y. B., Begum S., Lakhane M. A., Tiyyagura H. R., Khairnar R. S., and Bogle K. A. (**2021**) Nanostructured hydroxyapatite biomaterial as gas sensor. *Nanoscale Processing.*, 439-466.
5 Habraken W., Habibovic P., Epple M., and Bohner M. (**2016**) Calcium phosphates in biomedical applications : materials for the future ? *Mater. Today.*, 19 (2) 69-87.
6 Bezerra K. J. A., de Sena Silva I. N., Bezerra L. J. A., Cavalcante L. M. O., Amorim D. C., Machado D. P. J., Ximenes F. A. M. B., Almeida A. C. S., Costa L. V., Nunes N. V. A. A., and Valadas L. A. R. (**2020**) Biomedical Applications of Calcium Phosphate Ceramics as Biomaterials. *J. Young Pharm.*, 12 (3) 190-192.
7 Parent M., Baradari H., Champion E., and Damia C. (**2017**) Design of calcium phosphate ceramics for drug delivery applications in bone diseases : A review of the parameters affecting the loading and release of the therapeutic substance. *J. Control. Release.*, 252, 1-17.
8 Chatterjee S., Davies M. J., and Tarigopula G. (**2017**) Pharmacological control of blood sugar. *Anaesth. Intensive Care Med.*, 18 (10) 532-534.
9 Forlenza G. P., Buckingham B., and Maahs D. M. (**2016**) Progress in Diabetes Technology: Developments in Insulin Pumps, Continuous Glucose Monitors, and Progress towards the Artificial Pancreas. *J. Pediatr.*, 169, 13-20.
10 Gröning R., and Walz C. (**1995**) Development of experimental insulin pumps with glucose-controlled release. *Int. J. Pharm.*, 2 (119) 127-131.
11 El Rhilassi A., Mourabet M., El Boujaady H., Bennani-Ziatni M., El Hamri R., and Taitai A. (**2012)** Adsorption and release of amino acids mixture onto apatitic calcium phosphates analogous to bone mineral. *Appl. Surf. Sci.*, 259, 376-384.
12 El Rhilassi A., Mourabet M., Bennani-Ziatni M., El Hamri R., and Taitai A. (**2016**) Interaction of some essential amino acids with synthesized poorly crystalline hydroxyapatite. *J. Saudi Chem. Soc.*, 20, S632-S640.
13 Combes C., and Rey C. (**2002**) Adsorption of proteins and calcium phosphate materials bioactivity. *Biomaterials*, 23, 2817-2823.
14 Kandori K., Masunari A., and Ishikawa T. (**2005**) Study on adsorption mechanism of proteins onto synthetic calcium hydroxyapatites through ionic con- centration measurements. *Calcif Tissue Int.*, 76, 194-206.
15 Bennani-Ziatni M., Lebugle A., and Bonel G. (**1991**) Contribution à l'étude des apatites carbonatées déficientes en ions calcium : I-Synthèse et étude des coprécipités de phosphate de calcium carbonate de calcium après séchage. *Ann. Chim.Fr.*, 16, 607-617.
16 Monnier D., and Charlot G. (**1967**) Les méthodes de la chimie analytique : analyse quantitative minérale : 5ème Edition entièrement refondue, Masson et Cie, Paris, 1966, 1024 pp., Cartonné toile frs 135. *Anal. Chim. Acta.*,
17 Noh J. S., and Schwarz J. A. (**1989**) Estimation of the point of zero charge of simple oxides by mass titration. *J. Colloid Int Sci.*, 130 (1) 157-164.
18 Sarmento B., Ribeiro A., Veiga F., and Ferreira D. (**2006**) Development and characterization of new insulin containing polysaccharide nanoparticles. *Colloids Surf. B : Biointerfaces.*, 53 (2) 193-202.

19 Ye S., Li H., Yang W., and Luo Y. (**2014**) Accurate Determination of Interfacial Protein Secondary Structure by Combining Interfacial-Sensitive Amide I and Amide III Spectral Signals. *J. Am. Chem. Soc.*, 136 (4) 1206-1209.
20 Ji Y., Yang X., Ji Z., Zhu L., Ma N., Chen D., Jia X., Tang J., and Cao Y. (**2020**) DFT-Calculated IR Spectrum Amide I, II, and III Band Contributions of *N*-Methylacetamide Fine Components. *ACS Omega.*, 5 (15) 8572-8578.
21 Elhady O. M., Mansour E. S., Elwassimy M. M., Zawam S. A., Drar A. M., and Abdel-Raheem Sh. A. A. (**2022**) Selective synthesis, characterization, and toxicological activity screening of some furan compounds as pesticidal agents. *Curr. Chem. Lett.*, 11 (3) 285-290.
22 Langmuir I. (**1918**) The adsorption of gases on plane surfaces of glass, mica and platinum. *J. Am. Chem. Soc.*, 40 (9) 1361-1403.
23 Freundlich H. M. F. (**1906**) Über die adsorption in lösungen. *Z. Phys. Chem.*, 57, 385-470.
24 Elovich S. Y., and Larionov O. G. (**1962**) Theory of adsorption from nonelectrolyte solutions on solid adsorbents. *Russ. Chem. Bull.*, 11 (2) 198-203.
25 Temkin M. J., and Pyzhev V. (**1940**) Recent modifications to Langmuir Isotherms. *Acta. Physicochimie USSR.*, 12, 217-222.
26 Dubinin M. M., and Radushkevich L. V. (**1947**) Equation of the Characteristic Curve of Activated Charcoal. *J. Proc. Acad. Sci. USSR, Phys. Chem.*, 55, 331-333.
27 Weber T. W., and Chakravorti R. K. (**1947**) Pore and solid diffusion models for fixed-bed adsorbers. *AIChE J.*, 20 (2) 228-238.
28 Ho Y. S. (**2006**) Isotherms for the sorption of lead onto peat : Comparison of linear and non-linear methods. *Pol. J. Environ. Stud.*, 15 (1) 81–86.
29 Jiang L., Li S., Yu H., Zou Z., Hou X., and Shen F. (**2016**) Amino and thiol modified magnetic multi-walled carbon nanotubes for the simultaneous removal of lead, zinc, and phenol from aqueous solutions. *Appl. Surf. Sci.*, 369, 398-413.
30 Hall K. R., Eagleton L. C., Acrivos A., and Vermeulen T. (**1966**) Pore- and solid-diffusion kinetics in fixed-bed adsorption under constant-pattern conditions. *Ind. Eng. Chem. Fund.*, 5 (2) 212-223.
31 Helfferich F. (**1962**) Ion exchange. McGraw-Hill, New York, 335-360.
32 Dostert K-H., O'Brien C. P., Mirabella F., I-Barceló F., and Schauermann S. (**2016**) Adsorption of acrolein, propanal, and allyl alcohol on Pd(111): a combined infrared reflection–absorption spectroscopy and temperature programmed desorption
33 Yesilel O. Z., Olmez H., and Arici C. (**2007**) The first bis(orotato-*N*,*O*) cadmium complex with monodentate protonated ethylenediamine ligands: Synthesis, spectrothermal properties of a cadmium(II)-orotato complex with ethylenediamine – Crystal structure of trans-$[Cd(HOr)_2(enH)_2]\cdot 2H_2O$ and *cis*-$[Cd(H_2O)_2(phen)_2](H_2Or)_2\cdot 2H_2O$. *Polyhedron*, 26, 3669-3674.
34 Abdel-Raheem Sh. A. A., Kamal El-Dean A. M., Abd ul-Malik M. A., Hassanien R., El-Sayed M. E. A., Abd-Ella A. A., Zawam S. A., and Tolba M. S. (**2022**) Synthesis of new distyrylpyridine analogues bearing amide substructure as effective insecticidal agents. *Curr. Chem. Lett.*, 11 (1) 23-28.